

Computation of the latent heat of the deconfinement phase transition of SU(3) Yang-Mills theory

Luca Virzi,^{a,b,*} Leonardo Giusti,^{a,b} Mitsuaki Hirasawa^{a,b} and Michele Pepe^b

^aDepartment of Physics "G. Occhialini", University of Milan-Bicocca,
Piazza della Scienza 3, I-20126 Milano, Italy

^bINFN, Sezione di Milano-Bicocca,
Piazza della Scienza 3, I-20126 Milano, Italy

E-mail: l.virzi@campus.unimib.it, leonardo.giusti@mib.infn.it,
mitsuaki.hirasawa@mib.infn.it, michele.pepe@mib.infn.it

We investigate the thermal properties of SU(3) Yang-Mills theory across the deconfinement phase transition considering the framework of shifted boundary conditions in the temporal direction. By measuring the entropy density $s(T_c)/T_c^3$ on both sides of the phase transition at the critical temperature T_c , we can retrieve the latent heat h . Additionally, we compute h from the discontinuity in the trace anomaly of the energy-momentum tensor. Simulations are performed at five different values of the lattice spacing, allowing us to extrapolate the results to the continuum limit. The two observables produce compatible results, giving the combined estimate $h = 1.175(10)$ in the continuum limit, achieving a precision of about 1%. Moreover, we determine the critical temperature in physical units with permille accuracy, yielding $T_c \sqrt{t_0} = 0.24915(29)$. These results allow us to connect the confined and the deconfined phases with precision, and we present an improved computation of the Equation of State across the phase transition for temperatures between 0 and $3.4T_c$.

The 41st International Symposium on Lattice Field Theory (LATTICE2024)
28 July - 3 August 2024
Liverpool, UK

*Speaker

1. Introduction

Insights about the thermal properties of Quantum Chromodynamics (QCD) can be derived from a detailed investigation of its gauge sector, described by the SU(3) Yang-Mills theory. At variance with QCD that smoothly connects low and high temperatures, SU(3) Yang-Mills theory is characterized by a deconfinement phase transition. While the first order nature of the transition is well established, the latent heat h released during the transition is currently known with a precision of a few percent [1–4]. The latent heat is defined as the discontinuity in the energy density or, equivalently, in the entropy density, at the transition point between the confined and the deconfined phases. Within the conventional approach, h is retrieved from the discontinuity in the trace anomaly of the energy-momentum tensor $T_{\mu\nu}$ (EMT) at criticality. Notice that the trace anomaly is affected by an ultraviolet divergence related to the mixing with the identity operator, which anyway cancels out when computing its gap at the critical point. In this study we consider an alternative approach, where the latent heat is obtained from the discontinuity in the entropy density at the critical temperature. The implementation of shifted boundary conditions [5–7] represents a convenient framework where the thermal features can be studied very efficiently by Monte Carlo simulations [8, 9]. Finally, we present a computation of the Equation of State of the SU(3) Yang-Mills theory across the deconfinement phase transition [10], updating and complementing the results obtained in Ref. [9]. The determination of the Equation of State across the critical point provides a deeper understanding of the thermal features and of the phase transitions of a strongly interacting gauge theory, which may be relevant in the context of dark matter formation in the early Universe [11–13].

2. General setup and strategy

We formulate the SU(3) Yang-Mills theory on a (3+1)-dimensional lattice with size $L^3 \times L_0$ and lattice spacing a . Gauge fields are represented by link variables $U_\mu(x) \in \text{SU}(3)$, which satisfy periodic boundary conditions in the spatial direction and shifted boundary conditions along the temporal one:

$$U_\mu(L_0, \mathbf{x}) = U_\mu(0, \mathbf{x} - L_0 \boldsymbol{\xi}), \quad (1)$$

where $L_0 \boldsymbol{\xi}$ is a vector with integer components in lattice units. The Wilson gauge action is given by:

$$S[U] = \beta \sum_x \sum_{\mu < \nu} \left[1 - \frac{1}{3} \text{Re Tr}[U_{\mu\nu}(x)] \right], \quad (2)$$

where the trace is taken over the color index, $\beta = 6/g_0^2$ is the inverse of the bare coupling g_0^2 and $U_{\mu\nu}(x)$ is the plaquette field

$$U_{\mu\nu}(x) = U_\mu(x) U_\nu(x + a\hat{\mu}) U_\mu^\dagger(x + a\hat{\nu}) U_\nu^\dagger(x), \quad (3)$$

with x being the space-time coordinate, $\mu, \nu = 0, \dots, 3$ and $\hat{\mu}$ is the unit vector along the corresponding direction. In the thermodynamic limit, due to the invariance under Poincaré transformations [7], the system with shifted boundary conditions is equivalent to a system with periodic boundary conditions but temporal extent given by $L_0 \sqrt{1 + \boldsymbol{\xi}^2}$, which specifies the inverse temperature T^{-1} . In the framework of shifted boundary conditions, the off-diagonal elements of the energy-momentum

tensor are no longer all vanishing and we can define the entropy density $s(T)$ at the temperature T through the expectation value of the space-time components of the EMT $\langle T_{0k} \rangle_\xi$ [7]

$$\frac{s(T)}{T^3} = -\frac{(1 + \xi^2)}{\xi_k} \frac{Z_T \langle T_{0k} \rangle_\xi}{T^4}, \quad (4)$$

where the energy-momentum tensor on the lattice is defined as follows [14]

$$T_{\mu\nu} = \frac{\beta}{6} \left\{ F_{\mu\alpha}^a F_{\nu\alpha}^a - \frac{1}{4} F_{\alpha\beta}^a F_{\alpha\beta}^a \right\}. \quad (5)$$

The field strength tensor $F_{\mu\nu}(x) = F_{\mu\nu}^a(x) T^a$ on the lattice is given by

$$F_{\mu\nu}^a(x) = -\frac{i}{4a^2} \text{Tr} \left\{ [Q_{\mu\nu}(x) - Q_{\nu\mu}(x)] T^a \right\}, \quad (6)$$

with $T^a \in \mathfrak{su}(3)$ being the generators of the group SU(3), normalized as $2 \text{Tr} [T^a T^b] = \delta^{ab}$. The clover field $Q_{\mu\nu}(x)$ is defined as the sum of the four coplanar plaquettes resting on the lattice site x :

$$Q_{\mu\nu}(x) = U_{\mu\nu}(x) + U_{\nu-\mu}(x) + U_{-\mu-\nu}(x) + U_{-\nu\mu}(x), \quad (7)$$

with the minus sign standing for the negative direction.

The lattice regularization breaks explicitly the invariance of the theory under translations and rotations, hence the energy-momentum tensor on the lattice is not a conserved quantity. In order to have a lattice definition of the EMT that approaches the continuum one when $a/L \rightarrow 0$, $T_{\mu\nu}$ must be multiplicatively renormalized [14] and $Z_T(g_0^2)$ is the renormalization constant of the sextet component of the tensor. The renormalization constant in the pure SU(3) gauge theory has been computed non-perturbatively in [9, 15].

The latent heat is defined as the difference in the energy density - or, equivalently, in the entropy density - between the coexisting phases at criticality, hence the first step of this study consists in the determination of the critical temperature T_c . Then we perform two separate Monte Carlo simulations at T_c , where we compute the entropy density in the confined and deconfined phase, $s(T_c^-)$ and $s(T_c^+)$ respectively, and extrapolate their value to the continuum limit. The latent heat h is then given by

$$h = \frac{\Delta s(T_c)}{T_c^3} = \frac{s(T_c^+) - s(T_c^-)}{T_c^3}. \quad (8)$$

Alternatively, we can compute h from the discontinuity in the trace anomaly $A(T)$ of the EMT at the two sides of the phase transition. Using the definition related to the action density [16], we have

$$h = \frac{\Delta A(T_c)}{T_c^4} = \frac{d\beta}{d \log(a)} \frac{a^4}{\beta L_0 L^3} \frac{\langle S(T_c^+) \rangle - \langle S(T_c^-) \rangle}{T_c^4}, \quad (9)$$

where the dependence of the lattice spacing on the bare gauge coupling can be found in [17].

3. Determination of the critical coupling

We have performed Monte Carlo simulations at five different values of the lattice spacing, corresponding to systems with temporal extension $L_0/a = 5, 6, 7, 8$ and 9. In all cases we adopted

shifted boundary conditions with shift vector $\xi = (1, 0, 0)$, since for this value small lattice artifacts have been previously observed for $\langle T_{0k} \rangle_\xi$ [7, 8, 15]. Gauge configurations have been generated with the standard overrelaxed Cabibbo-Marinari algorithm [18, 19]. Close to criticality, Monte Carlo simulations show long autocorrelation times, thus we need large statistics - $\mathcal{O}(10^6)$ configurations - to obtain accurate numerical estimates. Various observables can be considered to define the critical coupling β_c , but they are all equivalent in the thermodynamic limit: in this study we use the quantity proposed in [20, 21], which shows a rapid convergence to the infinite volume value of β_c . In correspondence of first order phase transitions, an accurate determination of the critical coupling by numerical simulations at finite volume relies on a proper sampling of the coexisting phases, which can be obtained when many tunneling events occur in the Monte Carlo history. The probability of a tunneling event decays exponentially as the spatial size of the system increases, thus a fast convergence to the thermodynamic limit enables us to work with lattices with moderate spatial volumes.

At the deconfinement phase transition the \mathbb{Z}_3 center symmetry of the SU(3) Yang-Mills theory gets spontaneously broken: in the confined (cold) phase we have a single vacuum, while in the deconfined (hot) phase there are 3 degenerate vacua. The expectation value of the Polyakov loop $\langle \Phi \rangle$ is an order parameter of this transition, and it can be used to characterize the different phases. When shifted boundary conditions are taken into account, the \mathbb{Z}_3 center symmetry of the theory is unaffected. However, the usual definition of the Polyakov loop needs to be modified in order to guarantee gauge invariance, but it remains charged under that symmetry. We define the modified Polyakov loop for $\xi = (1, 0, 0)$ as follows

$$\Phi(\mathbf{x}) = \prod_{n=0}^{L_0/a-1} U_0(na, \mathbf{x}) \prod_{n=0}^{L_0/a-1} U_1(0, \mathbf{x}_n), \quad (10)$$

where $\mathbf{x}_n = \mathbf{x} - (L_0 - na)\xi$. It is useful to consider also the \mathbb{Z}_3 projection

$$\phi = \text{Re} \left\{ \frac{1}{(L/a)^3} \left(\sum_x \frac{1}{3} \text{Tr}[\Phi(\mathbf{x})] \right) \bar{z} \right\}, \quad (11)$$

with z being the SU(3) center element closest to the spatial average of $\text{Tr}[\Phi(\mathbf{x})]/3$. Close to the critical point, the probability distribution of ϕ exhibits two peaks corresponding to the confined and deconfined phases, separated by a minimum located at ϕ_0 . In a finite volume, however, the phase categorization of a field configuration is somehow conventional: if we label with ω_c and ω_d , respectively, the probability of finding the system in the confined or in the deconfined phase, the phase transition takes place when [20, 21]

$$\omega_d = 3\omega_c, \quad (12)$$

where the 3 factor on the r.h.s. is due to the 3-fold degeneracy of the vacuum in the deconfined phase. The numerical estimation of these statistical weights provides a reliable result only if both phases have been correctly sampled, namely if many tunneling events occurred during the simulation. Following [20], we can then define the two probabilities as:

$$\omega_c(\beta, L/a) = \langle \theta(\phi_0 - \phi) \rangle, \quad \omega_d(\beta, L/a) = \langle \theta(\phi - \phi_0) \rangle, \quad (13)$$

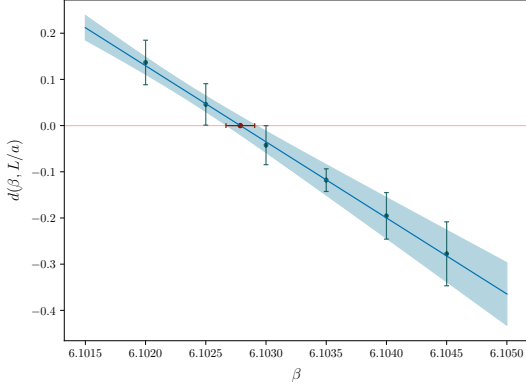


Figure 1: Dependence of $d(\beta, L/a)$ on β for $L_0/a = 6$ and $L/a = 48$. The critical coupling $\beta_c(L_0/a, L/a)$ - red horizontal point - is given by the zero-crossing of the linear fit function. The blue band represents a fit of the data.

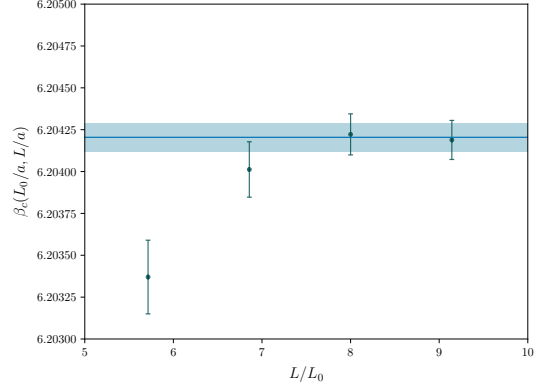


Figure 2: Dependence of $\beta_c(L_0/a, L/a)$ on L/L_0 for $L_0/a = 7$. The band represents the estimate of $\beta_c(L_0/a)$ coming from the weighted average of the data in the thermodynamic limit plateau, i.e. obtained at the two largest values of L/L_0 .

where θ is the Heaviside step function, and the local minimum ϕ_0 is found by means of a quartic fit in the region between the two peaks. Notice that with this approach the estimation of the statistical weights should be affected by finite-size effects which decay exponentially with the spatial extent of the lattice [20]. Hence on a finite lattice one can consider the quantity

$$d(\beta, L/a) = \frac{3\omega_c(\beta, L/a) - \omega_d(\beta, L/a)}{3\omega_c(\beta, L/a) + \omega_d(\beta, L/a)}, \quad (14)$$

which, by definition, vanishes when the criticality condition (12) is met. The critical coupling β_c is then retrieved through a finite-size scaling study: for a fixed lattice geometry, we compute the parameter $d(\beta, L/a)$ and define $\beta_c(L_0/a, L/a)$ from the zero-crossing of $d(\beta, L/a)$ through a linear interpolation of the collected data, see Figure 1 for an example with $L_0/a = 6$ and $L/a = 48$. Finally, the critical coupling is obtained by extrapolating $\beta_c(L_0/a, L/a)$ to the infinite volume limit, i.e. $\beta_c(L_0/a) = \lim_{L/a \rightarrow \infty} \beta_c(L_0/a, L/a)$. In Figure 2 we report an example for $L_0/a = 7$. Data show a rapid convergence to the infinite spatial volume limit, and the final result is estimated through a weighted average of the data points in the thermodynamic limit plateau. The estimated values of the critical coupling for $L_0/a = 5, 6, 7, 8$ and 9 are reported in Table 1. We can now express the critical temperature $aT_c = (a/L_0)/\sqrt{2}$ in physical units with high precision. We consider the gradient-flow time t_0 [22] to set the scale and we refer to the results in [17] to relate t_0/a^2 to the gauge coupling β . Lattice artifacts on $T_c\sqrt{t_0}$ are very small, and a linear extrapolation in $(a/L_0)^2$ to the continuum gives

$$T_c\sqrt{t_0} = 0.24915(29), \quad (15)$$

with a 1‰ final precision, mainly due to the uncertainty on the relation between t_0 and β . This estimate is in agreement with the analogous result in [4] in units of the scale w_0 , once that the relation between the two different scales is taken into account [23].

4. Latent heat

We compute the latent heat of the SU(3) Yang-Mills theory from the discontinuity between the confined and deconfined phases at T_c of both the entropy density and the trace anomaly. We unambiguously perform Monte Carlo simulations in either phase by considering lattices with very large spatial extent, so that the probability of a tunneling event to the other phase is negligible. The deconfined system is prepared by choosing an ordered field configuration as our initial condition, while the confined system is prepared by using a field configuration thermalized at $T < T_c$ as the starting point. Results are extrapolated to the continuum limit by considering values of $\Delta s(T_c)/T_c^3$ and $\Delta A(T_c)/T_c^4$ computed at five different lattice spacings $L_0/a = 5, 6, 7, 8$ and 9 , at the critical couplings reported in Table 1. In order to avoid additional finite-size effects due to shifted boundary conditions, the aspect ratio of each lattice must be an even integer number for $\xi = (1, 0, 0)$ - as it was pointed out in [7] - so we choose $L/a = 288$ for $L_0/a = 6, 8, 9$, while for $L_0/a = 5, 7$ we use $L/a = 280$. Moreover, finite volume effects are negligible with respect to the statistical uncertainty, given the large spatial volumes we employed [9]. In Figure 3 we display the dependence on $(a/L_0)^2$ of the entropy density in the confined phase (lower panel) and in the deconfined phase (upper panel), alongside with their continuum limit extrapolations. Lattice artifacts are small in the cold phase and moderate in the hot one, and data are well described by a linear fit in both cases, which give

$$\frac{s(T_c^-)}{T_c^3} = 0.2928(38), \quad \frac{s(T_c^+)}{T_c^3} = 1.471(16). \quad (16)$$

Consequently, as Figure 4 shows (red crosses), the lattice artifacts for h are moderate and data follow a linear behaviour in $(a/L_0)^2$. In Figure 4 we also show the continuum extrapolation of the latent heat measured from the discontinuity in the trace anomaly (blue dots), and overall we obtain

$$h = \frac{\Delta s(T_c)}{T_c^3} = 1.177(14), \quad h = \frac{\Delta A(T_c)}{T_c^4} = 1.173(11), \quad (17)$$

which result in the combined estimate $h = 1.175(10)$.

5. Equation of State

Using the data for the critical couplings $\beta_c(L_0/a)$ listed in Table 1 and the determination of T_c in units of $\sqrt{t_0}$ in Eq. (15), we have evaluated the entropy density and the pressure of the system for temperatures between 0 and $3.433 T_c$. Monte Carlo simulations have been carried out on lattices with spatial size $L/a = 280$ for $L_0/a = 5$ and 7 and with $L/a = 288$ for $L_0/a = 6$ and 8 , and all the results for the entropy density are reported in Table 3 of [10].

For temperatures $T/T_c \in [1, 3.433]$ we consider a Padé fit

$$\frac{s(T)}{T^3} = \frac{s_1 + s_2 w + s_3 w^2}{1 + s_4 w + s_5 w^2}, \quad (18)$$

where $w = \log(T/T_c)$. At the lowest investigated temperature, $T/T_c = 0.80$, data agrees with the expectation coming from a model based on a gas of non-interacting relativistic glueballs (see the red-dashed curve in Fig. 6), where the pressure given by a

L_0/a	$\beta_c(L_0/a)$
5	5.99115(4)
6	6.10285(8)
7	6.20420(8)
8	6.29626(12)
9	6.38017(16)

Table 1: Infinite volume limit of the critical coupling β_c for different lattice sizes.

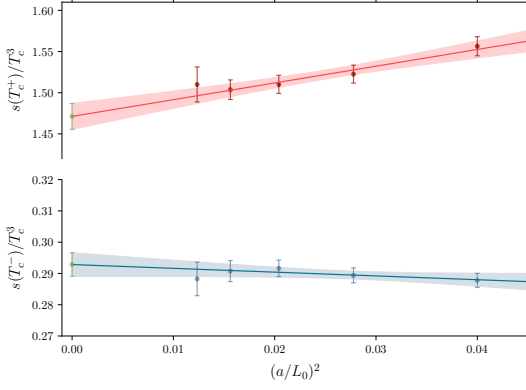


Figure 3: Extrapolation to the continuum limit of the entropy density: in the upper panel we show the deconfined phase, $s(T_c^+)/T_c^3$, while in the lower panel we show the confined phase, $s(T_c^-)/T_c^3$. The colored bands represent linear fits of the data.

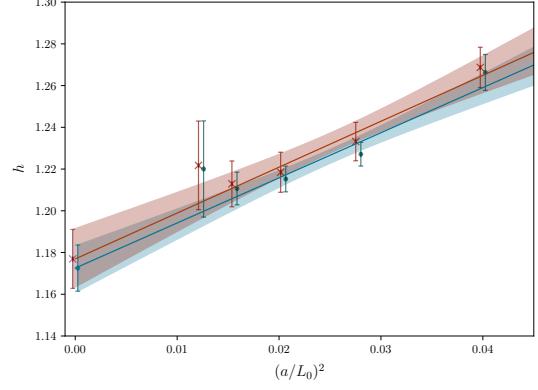


Figure 4: Extrapolation to the continuum limit of the latent heat h . Crosses (red) and dots (blue) represent, respectively, the data retrieved from Δs and ΔA . The bands represent linear fits of the data. Data have been slightly displaced to improve readability.

particle of mass m at temperature T is:

$$p(m, T) = (2J + 1) \frac{(mT)^2}{2\pi^2} \sum_{n=1}^{\infty} \frac{1}{n^2} K_2 \left(n \frac{m}{T} \right), \quad (19)$$

where K_2 is a modified Bessel function, and J is the spin of each particle. We have considered the four lightest glueball states $0^{++}, 0^{-+}, 2^{++}, 2^{-+}$ with mass lower than $2m_{0^{++}}$. Their masses, in units of $\sqrt{\sigma}$, are respectively 3.405(21), 5.276(45), 4.894(22), 6.32(9) [24]. These values can be expressed in units of T_c through the relation $T_c/\sqrt{\sigma} = 0.6462(30)$ [25] with the string tension σ . At higher temperatures heavier states contribute to the entropy density and the Hagedorn spectrum [26] describes how this can happen. Overall, a phenomenological fit $(a_0 + a_1 t^{1/3} + a_2 t^{2/3} + a_3 t)$, with $t = (1 - T/T_c)$, gives a good interpolation of our numerical results for $s(T)/T^3$ in the range $T/T_c \in [0.8, 1]$. Once that a convenient parametrization of the entropy density has been found, we can determine the pressure $p(T)$ by integrating $s(T)$ in the temperature. For temperatures in the range $T/T_c \in [0.8, 1]$ we can represent the pressure with a cubic fit function

$$\frac{p(T)}{T^4} = p_0 + p_1 t + p_2 t^2 + p_3 t^3, \quad (20)$$

while above T_c we parametrize the pressure with a Padé interpolant

$$\frac{p(T)}{T^4} = \frac{p_1 + p_2 w + p_3 w^2}{1 + p_4 w + p_5 w^2}. \quad (21)$$

Once that the entropy density and the pressure are known, we can retrieve the energy density from the thermodynamic relation $Ts = \varepsilon + p$. In Figure 5 we show the dependence of these thermodynamic potentials on the temperature in the range $T/T_c \in [0.8, 3.433]$. In Figure 6 we show more closely the behaviour of the entropy density and of the pressure near the phase transition, alongside the non-interacting glueball gas prediction. All the reported results have been extrapolated to the

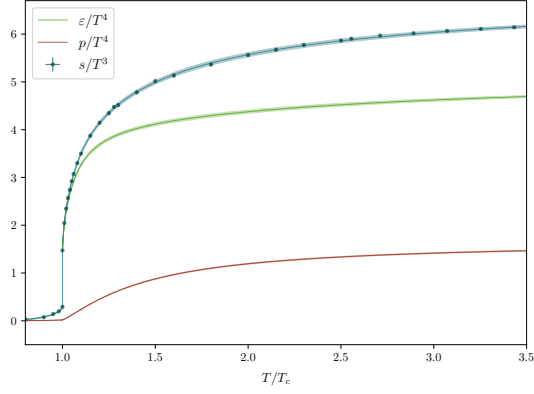


Figure 5: Dependence of the potentials $s(T)/T^3$ (blue, top), $\varepsilon(T)/T^4$ (green, middle) and $p(T)/T^4$ (red, bottom) on T/T_c in the range $T/T_c \in [0.8, 3.433]$. Bands represent the interpolating functions described in Section 5.

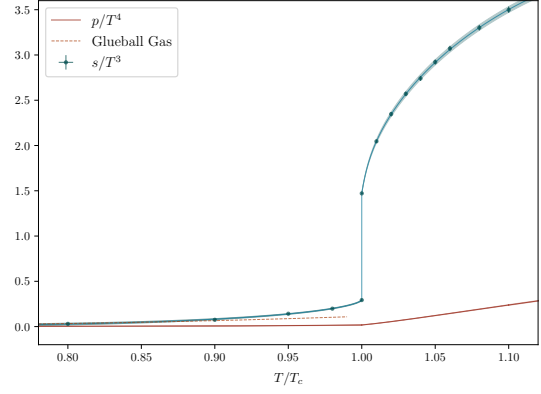


Figure 6: Detail of the dependence of $s(T)/T^3$ and $p(T)/T^4$ in the range $T/T_c \in [0.8, 1.1]$, alongside the non-interacting glueball gas expectation (red-dashed curve).

continuum, and the details of each parametrization can be found in [10]. With this computation of the Equation of State of the SU(3) Yang-Mills theory across the deconfinement phase transition we complement the results obtained in Ref. [9].

6. Conclusions

We explored the thermal properties of the SU(3) Yang-Mills theory across the deconfinement phase transition in the framework of shifted boundary conditions. We determined the critical temperature T_c in physical units with a permille precision, yielding $T_c \sqrt{t_0} = 0.24915(29)$, then we computed the latent heat from the discontinuity of both the entropy density and the trace anomaly at criticality. A combined estimate in the infinite spatial volume and continuum limit gives $h = 1.175(10)$, with a precision of about 1%. This result is in tension with the current best estimate [4] of h , while it is consistent with the result quoted in [3] for a fixed aspect ratio. Finally, we performed a precise determination of the Equation of State of the SU(3) Yang-Mills theory across the deconfinement phase transition, complementing the results of Ref. [9].

Acknowledgments

We acknowledge YITP in Kyoto University for granting us access to the supercomputer Yukawa-21. We also thank CINECA for providing us with a very generous access to Leonardo during the early phases of operations of the machine and for the computer time allocated thanks to CINECA-INFN and CINECA-Bicocca agreements. The R&D has been carried out on the PC clusters Wilson and Knuth at Milano-Bicocca. This work is (partially) supported by ICSC - Centro Nazionale di Ricerca in High Performance Computing, Big Data and Quantum Computing, funded by European Union - NextGenerationEU. We wish to thank Leonardo Cosmai for useful discussions and Isabella Leone Zimmer for her contribution during the early stages of this collaboration.

References

- [1] S. Borsanyi, Z. Fodor, C. Hoelbling, S.D. Katz, S. Krieg and K.K. Szabo, *Full result for the QCD equation of state with 2+1 flavors*, *Phys. Lett. B* **730** (2014) 99 [1309.5258].
- [2] M. Shirogane, S. Ejiri, R. Iwami, K. Kanaya and M. Kitazawa, *Latent heat at the first order phase transition point of $SU(3)$ gauge theory*, *Phys. Rev. D* **94** (2016) 014506 [1605.02997].
- [3] WHOT-QCD collaboration, *Latent heat and pressure gap at the first-order deconfining phase transition of $SU(3)$ Yang-Mills theory using the small flow-time expansion method*, *PTEP* **2021** (2021) 013B08 [2011.10292].
- [4] S. Borsanyi, K. R., Z. Fodor, D.A. Godzieba, P. Parotto and D. Sexty, *Precision study of the continuum $SU(3)$ Yang-Mills theory: How to use parallel tempering to improve on supercritical slowing down for first order phase transitions*, *Phys. Rev. D* **105** (2022) 074513 [2202.05234].
- [5] L. Giusti and H.B. Meyer, *Thermodynamic potentials from shifted boundary conditions: the scalar-field theory case*, *JHEP* **11** (2011) 087 [1110.3136].
- [6] L. Giusti and H.B. Meyer, *Thermal momentum distribution from path integrals with shifted boundary conditions*, *Phys. Rev. Lett.* **106** (2011) 131601 [1011.2727].
- [7] L. Giusti and H.B. Meyer, *Implications of Poincare symmetry for thermal field theories in finite-volume*, *JHEP* **01** (2013) 140 [1211.6669].
- [8] L. Giusti and M. Pepe, *Equation of state of a relativistic theory from a moving frame*, *Phys. Rev. Lett.* **113** (2014) 031601 [1403.0360].
- [9] L. Giusti and M. Pepe, *Equation of state of the $SU(3)$ Yang–Mills theory: A precise determination from a moving frame*, *Phys. Lett. B* **769** (2017) 385 [1612.00265].
- [10] L. Giusti, M. Hirasawa, M. Pepe and L. Virzì, *A precise study of the $SU(3)$ Yang-Mills theory across the deconfinement transition*, 2501.10284.
- [11] K.K. Boddy, J.L. Feng, M. Kaplinghat and T.M.P. Tait, *Self-Interacting Dark Matter from a Non-Abelian Hidden Sector*, *Phys. Rev. D* **89** (2014) 115017 [1402.3629].
- [12] A. Soni and Y. Zhang, *Hidden $SU(N)$ Glueball Dark Matter*, *Phys. Rev. D* **93** (2016) 115025 [1602.00714].
- [13] M. Laine, S. Procacci and A. Rogelj, *Evolution of coupled scalar perturbations through smooth reheating. Part I. Dissipative regime*, *JCAP* **10** (2024) 040 [2407.17074].
- [14] S. Caracciolo, G. Curci, P. Menotti and A. Pelissetto, *The Energy Momentum Tensor for Lattice Gauge Theories*, *Annals Phys.* **197** (1990) 119.
- [15] L. Giusti and M. Pepe, *Energy-momentum tensor on the lattice: Nonperturbative renormalization in Yang-Mills theory*, *Phys. Rev. D* **91** (2015) 114504 [1503.07042].

- [16] G. Boyd, J. Engels, F. Karsch, E. Laermann, C. Legeland, M. Lutgemeier et al., *Thermodynamics of $SU(3)$ lattice gauge theory*, *Nucl. Phys. B* **469** (1996) 419 [[hep-lat/9602007](#)].
- [17] L. Giusti and M. Lüscher, *Topological susceptibility at $T > T_c$ from master-field simulations of the $SU(3)$ gauge theory*, *Eur. Phys. J. C* **79** (2019) 207 [[1812.02062](#)].
- [18] N. Cabibbo and E. Marinari, *A New Method for Updating $SU(N)$ Matrices in Computer Simulations of Gauge Theories*, *Phys. Lett. B* **119** (1982) 387.
- [19] M. Creutz, *Monte Carlo Study of Quantized $SU(2)$ Gauge Theory*, *Phys. Rev. D* **21** (1980) 2308.
- [20] A. Francis, O. Kaczmarek, M. Laine, T. Neuhaus and H. Ohno, *Critical point and scale setting in $SU(3)$ plasma: An update*, *Phys. Rev. D* **91** (2015) 096002 [[1503.05652](#)].
- [21] C. Borgs, R. Kotecky and S. Miracle-Sole, *Finite size scaling for Potts models*, *J. Stat. Phys.* **62** (1991) 529.
- [22] M. Lüscher, *Properties and uses of the Wilson flow in lattice QCD*, *JHEP* **08** (2010) 071 [[1006.4518](#)].
- [23] ALPHA collaboration, *Power corrections from decoupling of the charm quark*, *Phys. Lett. B* **774** (2017) 649 [[1706.04982](#)].
- [24] A. Athenodorou and M. Teper, *$SU(N)$ gauge theories in 3+1 dimensions: glueball spectrum, string tensions and topology*, *JHEP* **12** (2021) 082 [[2106.00364](#)].
- [25] B. Lucini, M. Teper and U. Wenger, *The High temperature phase transition in $SU(N)$ gauge theories*, *JHEP* **01** (2004) 061 [[hep-lat/0307017](#)].
- [26] R. Hagedorn, *Statistical thermodynamics of strong interactions at high-energies*, *Nuovo Cim. Suppl.* **3** (1965) 147.